



HAL
open science

On the application of scintillometry over heterogeneous grids

J. Ezzahar, Ghani Chehbouni, Joost Hoedjes, Ah Chehbouni

► **To cite this version:**

J. Ezzahar, Ghani Chehbouni, Joost Hoedjes, Ah Chehbouni. On the application of scintillometry over heterogeneous grids. *Journal of Hydrology*, 2007, 334 (3-4), pp.493-201. 10.1016/j.jhydrol.2006.10.027 . ird-00389712

HAL Id: ird-00389712

<https://ird.hal.science/ird-00389712>

Submitted on 29 May 2009

HAL is a multi-disciplinary open access archive for the deposit and dissemination of scientific research documents, whether they are published or not. The documents may come from teaching and research institutions in France or abroad, or from public or private research centers.

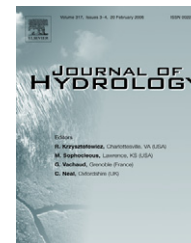
L'archive ouverte pluridisciplinaire **HAL**, est destinée au dépôt et à la diffusion de documents scientifiques de niveau recherche, publiés ou non, émanant des établissements d'enseignement et de recherche français ou étrangers, des laboratoires publics ou privés.



available at www.sciencedirect.com



journal homepage: www.elsevier.com/locate/jhydrol



2 On the application of scintillometry 3 over heterogeneous grids ☆

4 J. Ezzahar ^a, A. Chehbouni ^{b,*}, J.C.B. Hoedjes ^b, Ah. Chehbouni ^a

5 ^a Physics Department LMFE, Faculty of Sciences Semlalia, Marrakech, Morocco

6 ^b Centre d'Etudes Spatiales de la Biosphère (CESBIO), 18 Avenue Edouard Belin, 31401 Toulouse Cedex 9, France

Received 2 December 2005; received in revised form 13 October 2006; accepted 20 October 2006

KEYWORDS

Scintillation;
Eddy covariance;
Heterogeneity;
Aggregation;
Structure parameter

Summary In this paper the applicability of the Monin–Obukhov similarity theory (MOST) over heterogeneous terrain below the blending height is investigated. This is tested using two large aperture scintillometers (LAS), in conjunction with aggregation schemes to infer area-averaged refractive index structure parameters. The two LAS were operated simultaneously over the oliveyard of Agdal, located near Marrakech (Morocco). The Agdal olive yard is made up of two contrasted fields, or patches. The two sites are relatively homogeneous, but differ strongly in characteristics (mainly soil moisture status, and, to a lesser extent, vegetation cover). The higher soil moisture in the northern site creates heterogeneity at the scale of the entire olive yard (i.e. at grid scale). At patch scale, despite the complexity of the surface (tall, sparse trees), a good agreement was found between the sensible heat fluxes obtained from eddy-covariance systems and those estimated from the LAS. At grid scale, the aggregated structure parameter of the refractive index, simulated using the proposed aggregation model, behaves according to MOST. This aggregated structure parameter of the refractive index is obtained from measurements made below the grid scale blending height, and shows that MOST applies here. Consequently, scintillometers can be used at levels below the blending height. This is of interest, since strictly respecting the height requirements poses tremendous practical problems, especially if one is aiming to derive surface fluxes over large areas.

© 2006 Published by Elsevier B.V.

Introduction

The structure parameter of the refractive index (C_n^2) of air is a key parameter that characterizes the intensity of the turbulent fluctuations of the atmospheric refractive index. Using the scintillation technique, one can measure this parameter at spatial scales varying from several hundreds

☆ We, the authors, declare that the presented paper contains original work, is not being submitted elsewhere, and all authors agree to the contents and submission of the paper.

* Corresponding author. Tel.: +33 561 558 197; fax: +33 561 558 500.

E-mail address: ghani@cesbio.cnes.fr (A. Chehbouni).

18 of meters (e.g. displaced-beam laser scintillometer) up to
19 10 km (e.g. extra large aperture scintillometer). Depending
20 on the wavelength at which the scintillometer operates,
21 knowledge of C_n^2 permits the calculation of vertical fluxes
22 of heat or water vapour from the earth's surface, which
23 are required in many meteorological, hydrological and agri-
24 cultural applications. These fluxes can be, and have been,
25 measured using point-sampling measurement devices such
26 as Bowen-ratio or eddy-covariance (EC) systems. However,
27 for several applications, in particular large scale irrigation
28 management or the validation of surface parameterization
29 schemes in large-scale hydro-atmospheric models, grid-
30 scale values are required. A network of point-sampling de-
31 vices, such as eddy-covariance, can be used. However, the
32 high cost and the requirement of continuous availability of
33 well-trained staff to operate and maintain them has led
34 the scientific community to look for alternative techniques
35 to estimate area-averaged fluxes over large heterogeneous
36 surfaces.

37 In this context, a number of different techniques have
38 been introduced for research applications, such as a dis-
39 persometer theodolite, displaced-beam laser scintillome-
40 ters, microwave scintillometers and large or extra large
41 aperture scintillometers (LAS, XLAS). In this study we focus
42 on the scintillation technique. The principle of scintillome-
43 try consists of transmitting a beam of electromagnetic radi-
44 ation and measuring the intensity variations of the received
45 signal. Wang et al. (1978) have shown that the variance of
46 the logarithm of the intensity fluctuations can be related
47 to C_n^2 , which, for scintillometers operating at visible or
48 near-infrared wavelengths, can then be related to the struc-
49 ture parameter of temperature, C_T^2 , to derive the sensible
50 heat flux through Monin–Obukhov similarity theory (MOST)
51 (Wesely, 1976; Moene, 2003). Due to its ability to integrate
52 atmospheric processes along a transect, varying from a few
53 hundreds of metres up to a several kilometres, the scintilla-
54 tion method is a promising approach for routine observa-
55 tions of surface fluxes. Compared to e.g. eddy-covariance
56 systems, the scintillometer is easy to install, relatively
57 cheap and it is a practical method to obtain area-average
58 surface fluxes over several kilometres. The instrument is
59 capable of continuous measurements with minimum human
60 intervention.

61 Over the last decade, several authors have proven the
62 reliability of heat flux estimates from scintillometer over
63 fairly homogeneous terrain (e.g. Green et al., 1994; de
64 Bruin et al., 1995; Meijninger and de Bruin, 2000; Hoedjes
65 et al., 2002). Recently, several investigations have demon-
66 strated the potential of this method over moderately inho-
67 mogeneous surfaces (Chehbouni et al., 1999, 2000b; Beyrich
68 et al., 2002; Meijninger et al., 2002). However, a disadvan-
69 tage of the method is that it requires the use the semi-
70 empirical Monin–Obukhov similarity theory which might
71 not be applicable over very complex surfaces (Lagouarde
72 et al., 2002).

73 The main objective of this paper is to test the applicabil-
74 ity of MOST at grid scale. The grid consists of two or more
75 distinct fields (or patches) with different characteristics,
76 creating a heterogeneous (grid) surface. This is tested by
77 combining LAS measurements, over two individually homo-
78 geneous patches with different characteristics, with aggre-
79 gation schemes to derive a grid scale average refractive

index structure parameter, $\langle C_n^2 \rangle$ (angular brackets denoting
80 grid scale averages). The aggregation scheme is required
81 since C_n^2 is not linear. Regarding the aggregation issue, we
82 have adopted the deterministic approach (Shuttleworth,
83 1991; Arain et al., 1996; Noilhan and Lacarrere, 1995; Che-
84 hbouni et al., 1995, 2000a; Lagouarde et al., 2002), which
85 consists of deriving analytical relationships between local
86 and effective (area-averaged) surface parameters by
87 matching the model equations at different scales. In order
88 to develop the aggregation scheme and to verify the appli-
89 cability of the Monin–Obukhov similarity theory (MOST), a
90 field experiment has been designed and carried out during
91 the autumn of 2002 over the olive yard of Agdal in Morocco,
92 within the framework of the SUDMED (Chehbouni et al.,
93 2003) and IRRIMED projects (<http://www.irrimed.org>).
94

95 This paper is organized as follows: in “Theoretical back-
96 ground” section, the basic equations and the associated
97 procedure that allow the estimation of sensible heat flux
98 from the structure parameter of the refractive index of
99 air are presented. An overview of the experimental design
100 is outlined in “Experimental site and measurements” sec-
101 tion. In “Aggregation procedures for obtaining grid aver-
102 aged C_n^2 ” section, we present the developed aggregation
103 scheme to derive the area-averaged refractive index struc-
104 ture parameter $\langle C_n^2 \rangle$ over two adjacent olive tree fields un-
105 der unstable conditions. In “Results and discussion”
106 section, a comparison between LAS and EC derived mea-
107 surements at both patch and at grid scales is presented
108 (where patch scale refers to individual fields and grid scale
109 to the ensemble of several (in our case two) fields). Finally,
110 we conclude by discussing the accuracy of the suggested
111 approach to estimate the area-averaged structure parame-
112 ter of the refractive index and the applicability of MOST
113 at grid scale using measurements made below the blending
114 height.

Theoretical background

The large aperture scintillometer (LAS) is a device that mea-
115 sures the structure parameter of the refractive index of air.
116 In the optical domain, this C_n^2 depends mainly on tempera-
117 ture fluctuations and, to a lesser effect, humidity fluctua-
118 tions. Assuming that temperature and humidity fluctua-
119 tions are perfectly correlated, Wesely (1976) showed
120 that, to a good approximation, the temperature structure
121 parameter C_T^2 can be derived from C_n^2 by:

$$C_T^2 = C_n^2 \left(\frac{T^2}{\gamma P} \right)^2 \left(1 + \frac{0.03}{\beta} \right)^{-2}, \quad (1)$$

126 where γ is the refractive index coefficient for air
127 ($7.8 \times 10^{-7} \text{ K Pa}^{-1}$), and β the Bowen ratio. The final bracket-
128 ed term is a correction for the effects of humidity. C_n^2 and
129 C_T^2 are in ($\text{m}^{-2/3}$) and ($\text{K}^2 \text{ m}^{-2/3}$), respectively.
130

131 According to MOST, it is possible to link C_T^2 and the tem-
132 perature scale T_* for unstable conditions, i.e., $L < 0$ (de
133 Bruin et al., 1993) using:

$$\frac{C_T^2}{T_*^2(z-d)^{-2/3}} = f((z-d)/L) = 4.9(1-9(z-d)/L)^{-2/3}, \quad (2)$$

136 L is the Monin–Obukhov length defined as: 137

138

140
$$L = -\frac{T_a u_*^2}{\kappa g T_*} \quad (3)$$

141 with $\kappa = 0.41$, $g = 9.81 \text{ m s}^{-2}$ and u_* is the friction velocity,
142 given by:

143
$$u_* = \kappa u [\ln((z-d)/z_0) - \psi((z-d)/L)]^{-1}, \quad (4)$$

146 where ψ is the integrated stability function (Panofsky and
147 Dutton, 1984), z is the measurement height, d the displace-
148 ment height and z_0 is the roughness length.149 The sensible heat flux H (W m^{-2}) is calculated iteratively
150 using Eqs. (1)–(4) and the following relationship:

151
$$H = \rho c_p u_* T_* \quad (5)$$

154 where ρ (kg m^{-3}) and c_p ($\text{J kg}^{-1} \text{K}^{-1}$) are the air density and
155 specific heat capacity at constant pressure, respectively.

156 Experimental site and measurements

157 The experiment was carried out in the fall of 2002, between
158 day of year (DOY) 295 and 306 (22nd October–2nd Novem-
159 ber) at the 275 ha Agdal olive orchard, which is located to
160 the southeast of the city of Marrakech, Morocco ($31^\circ 36' \text{N}$,
161 $07^\circ 59' \text{W}$). The climate is semiarid Mediterranean. Precipita-
162 tion falls mainly during winter and spring, from the begin-
163 ning of November until the end of April, with an average
164 yearly rainfall of 175–250 mm. The atmosphere is very
165 dry, with an average humidity of 50%, and the potential
166 evaporation is very high (1600 mm per year), greatly
167 exceeding the annual rainfall. The experimental area is di-
168 vided in two fields, which are referred to as the southern
169 site and the northern site. The average height of the olive
170 trees is 6.5 m in the southern and 6 m in the northern site.
171 The vegetation is more homogenous in the southern site
172 than in the northern site, as can be seen in Fig. 1, with an
173 average vegetation cover of approximately 55% in the south-
174 ern site and 45% in the northern site, as obtained from hemi-
175 spherical canopy photographs (using a Nikon Coolpix 950[®]
176 with a FC-E8 fish-eye lens converter, field of view 183°).
177 The period of the experiment was chosen in order to have
178 a distinct difference between the two sites in term of soil
179 moisture. The southern site was dry and the northern site
180 had just been irrigated. Fig. 2 shows the evolution of the
181 volumetric water content throughout the experiment. From
182 Fig. 2, it is clear that the grid, comprised of the northern
183 and southern sites, is heterogeneous.

184 Both sites were equipped with a set of standard meteorol-
185 ogical instruments to measure wind speed and direction
186 (Young Wp200) and air temperature and humidity, using
187 HMP45AC temperature and humidity probes (Vaisala) at
188 9 m. Furthermore, net radiation in the southern site was
189 measured using a CNR1 (Kipp and Zonen) installed at 8 m
190 and Q7 net radiometer (REBS) at 7 m. In the northern site
191 the net radiation was measured with a Q6 net radiometer
192 (REBS) at 8 m. Net radiation over the soil in both fields
193 was measured by a Q7 at 1 m. Soil heat flux was measured
194 at three locations at a depth of 0.01 m using soil heat flux
195 plates (Hukseflux). The first was located below the canopy
196 close to the trunk of a tree, in order to be not exposed to
197 solar radiation; the second was exposed directly to solar
198 radiation, and the third was installed in an intermediate po-
199 sition, partly sunlit, partly shaded. An average of these

three measurements was calculated to obtain a representa-
200 tive value. Soil moisture was measured at different depths
201 (0.05, 0.1, 0.2, 0.3 and 0.4 m) using 5 CS616 water content
202 reflectometers (Campbell Scientific Ltd.). All meteorologi-
203 cal measurements were sampled at 1 Hz, and 30 min aver-
204 ages were stored. The prevailing wind direction is from
205 the northwest.
206

In both the northern and the southern site, EC systems
207 were installed to provide continuous measurements of the
208 vertical fluxes of heat, water vapour and CO_2 at a height
209 of 8.8 and 8.7 m for the southern and northern sites, respec-
210 tively. The EC systems consisted of a 3D sonic anemometer
211 (CSAT3, Campbell Scientific Ltd.) and an open-path infrared
212 gaz analyzer (Li7500, Licor Inc.). Raw data were sampled at
213 a rate of 20 Hz and were recorded using CR23X dataloggers
214 (Campbell Scientific Ltd.) which were connected to portable
215 computers to enable storage of large raw data files. The
216 half-hourly values of fluxes were later calculated off-line
217 after performing coordinate rotation, frequency correc-
218 tions, correcting the sonic temperature for the lateral
219 velocity and presence of humidity, and the inclusion of
220 the mean vertical velocity according to Webb et al.
221 (1980). Data from the eddy-covariance system were pro-
222 cessed using the software 'ECPack' developed by the Mete-
223 orology and Air Quality group, Wageningen University
224 (available for download at <http://www.met.wau.nl/>).
225

Air pressure was measured in the southern site using the
226 pressure sensor of the Li7500 infrared gas analyzer, and on
227 the northern site using a pressure sensor (Vaisala PTB101B).
228 1 min averages were recorded on the dataloggers.
229

The LAS operated in this study were built by the Mete-
230 orology and Air Quality Group (Wageningen University, the
231 Netherlands). These instruments have been constructed
232 according to the basic design described in Ochs and Wilson
233 (1993). They have an aperture size of 0.15 m and the trans-
234 mitter operates at a wavelength of 0.94 μm . At the receiver,
235 C_n^2 is sampled at 1 Hz and averaged over 1 min
236 intervals by a CR510 datalogger. Two identical LAS were
237 used in this experiment. The first was installed over the
238 southern site, perpendicular to the dominant wind direc-
239 tion, over a pathlength of 1050 m (denoted LAS_s). The trans-
240 mitter was mounted on a tripod installed on a roof, located
241 on the southwest corner of the southern site, while the re-
242 ceiver was mounted on a 15 m high tower that was posi-
243 tioned next to the road that separates the two sides of
244 the orchard. The second LAS was installed over the northern
245 site, the orientation of this LAS was almost parallel to the
246 dominant wind direction, and it measured over a pathlength
247 of 1070 m (denoted LAS_n). The receiver was installed on the
248 same tower as the receiver of LAS_s. The transmitter was
249 mounted on a tripod installed on a roof located near the
250 northern corner of the northern site. The setup of the
251 receivers on the 15 m tower was such that the two signals
252 did not interfere. The average heights of the LAS transects
253 were 14 m for the southern site and 14.5 m for the northern
254 site.
255

From Fig. 1 it can be seen that the two experimental
256 sites, especially the northern site, are not completely
257 homogeneous; intersecting dirt roads and missing trees
258 cause a certain degree of heterogeneity. However, consid-
259 ering the horizontal scale of these heterogeneities, the
260 experimental setup of both the EC systems and the LAS
261

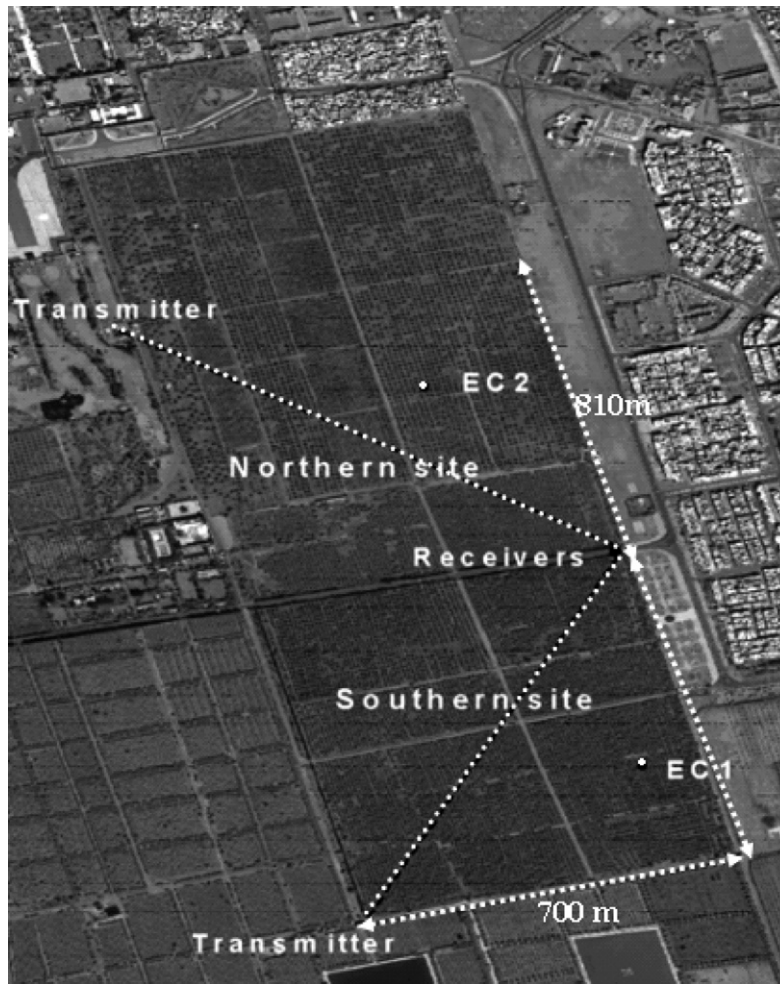


Figure 1 Overview of the experimental site (Quickbird image).

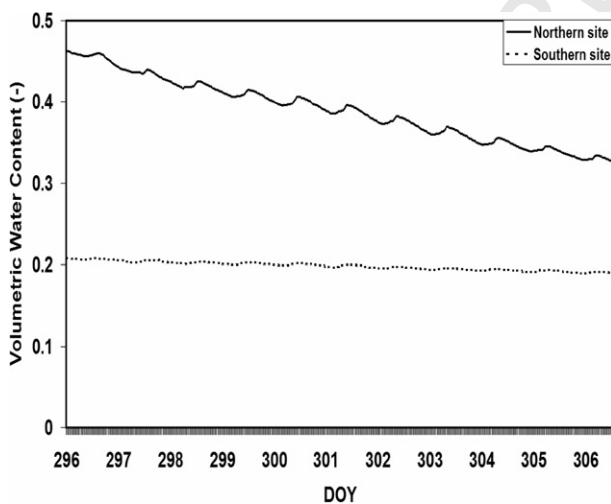


Figure 2 Evolution of the volumetric water content during the experimental period for the southern site (dotted line) and northern site (solid line).

is generally accepted to be applicable (Meijninger et al., 2002). In this study, patch scale refers to either northern or southern site, whereas grid scale refers to the entire oliveyard (or, the ensemble of northern and southern sites).

Aggregation procedures for obtaining grid averaged C_n^2

Due to the non-linearity of C_n^2 , the grid-scale average refractive index structure parameter $\langle C_n^2 \rangle$ cannot be obtained as a weighted average of the patch-scale C_n^2 values. Two alternative approaches are described in this section: the effective approach (denoted by subscript 'eff') and the aggregational approach (denoted by subscript 'agg'). In the effective approach, values of $\langle C_n^2 \rangle_{\text{eff}}$ are obtained through the combination of eddy correlation based measurements of H , $L_v E$, and u , and MOST. In the aggregated approach, $\langle C_n^2 \rangle_{\text{agg}}$ is obtained through a combination of MOST, an aggregation scheme and the LAS-based patch-scale measurements of C_n^2 .

Effective approach

The effective approach consists of deriving an area-averaged C_n^2 from eddy-covariance measurements. This $\langle C_n^2 \rangle_{\text{eff}}$ is obtained by inverting Eqs. (1)–(5) using grid

262 are believed to be at or above the blending height, or the
263 height at which the turbulent signatures of the individual
264 heterogeneous structures are mixed, and above which MOST

286 scale averages of sensible and latent heat fluxes and friction
287 velocity. $\langle H_{EC} \rangle_{\text{eff}}$ and $\langle LvE_{EC} \rangle_{\text{eff}}$ are obtained as a simple lin-
288 ear weighted average of the fluxes measured at both sites.
289 The effective friction velocity, $\langle u_{*EC} \rangle_{\text{eff}}$, is obtained by
290 applying the matching rule to momentum fluxes (Chehbouni
291 et al., 1999):
292

$$294 \langle u_{*EC} \rangle_{\text{eff}} = \left(\sum f_{iEC} u_{*iEC}^2 \right)^{0.5}, \quad (6)$$

295 where f_{iEC} is the fraction of the surface covered by the
296 patch i . Since the eddy-covariance systems at both northern
297 and southern sites were installed at approximately the same
298 height above the vegetation, we found it safe to assume
299 $f_{iEC} = 0.5$, since the size of the area from which the mea-
300 sured flux emanates will be roughly the same for each site.

301 Aggregational approach

302 The second approach consists of estimating a grid scale
303 average C_n^2 from the LAS measurements. This $\langle C_{nLAS}^2 \rangle_{\text{agg}}$ is
304 obtained using C_{ns}^2 and C_{nN}^2 in combination with the aggrega-
305 tion scheme described in this section. After obtaining a
306 patch scale sensible heat flux from each LAS (using Eqs.
307 (1)–(5)), a grid-scale sensible heat flux can be obtained as
308 follows:
309

$$311 \langle H \rangle = f_c H_{LAS,S} + (1 - f_c) H_{LAS,N}, \quad (7)$$

312 where subscripts S and N indicate variables associated with
313 the southern or northern site, respectively, and f_c is the
314 fraction of the southern area in the entire grid surface.
315 The value of f_c is further discussed in “grid scale” section
316 Eqs. (6) and (7) can be simplified as:
317

$$319 \langle u_* T_* \rangle = f_c u_{*S} T_{*S} + (1 - f_c) u_{*N} T_{*N}, \quad (8)$$

$$321 \langle u_*^2 \rangle = f_c u_{*S}^2 + (1 - f_c) u_{*N}^2. \quad (9)$$

322 According to Monin–Obukhov similarity theory and using the
323 scaling constants found by de Bruin et al. (1993):
324

$$326 \frac{C_n^2(z-d)^{2/3}}{T_*^2} = 4.9 \left(1 - 9 \frac{(z-d)}{L} \right)^{-2/3}. \quad (10)$$

327 By substituting Eq. (1) into Eq. (10) and Eq. (10) into (8), Eq.
328 (11) can be obtained:
329

$$331 \langle C_{nLAS}^2 \rangle_{\text{agg}} = \langle y \rangle^{-1} (y_S C_{ns}^2 + y_N C_{nN}^2) \quad (11)$$

332 with:

$$334 y_X = (f_X) \frac{u_{*X} \left(1 + \frac{0.03}{\beta_X} \right)^{-2} (z_X - d_X)^{2/3}}{T_{*X} \left(1 - 9 \frac{(z_X - d_X)}{L_X} \right)^{-2/3}}, \quad (12)$$

335 where X is either S, N or indicating the grid-scale average
336 (angular brackets), and $f_X = 1$ for $\langle y \rangle$, $f_X = f_c$ for y_S and
337 $f_X = (1 - f_c)$ for y_N . Using once again the principle that con-
338 sists of formulating grid-scale surface fluxes using the same
339 equations that govern the patch-scale behaviour, but whose
340 arguments are the aggregate expressions of those at the
341 patch-scale (Chehbouni et al., 2000a), $\langle L \rangle$ is derived from
342 the area-average sensible heat flux and friction velocity as :

$$344 \langle L \rangle = \frac{-\rho c_p T_a \langle u_* \rangle^3}{kg(H)}, \quad (13)$$

$\langle \beta \rangle$ is the grid-scale average Bowen ratio, defined as:

$$\langle \beta \rangle = \frac{\langle H \rangle}{\langle LvE \rangle}, \quad (14)$$

where $\langle LvE \rangle$ is defined analogous to $\langle H \rangle$ in Eq. (7), with
patch scale values of LvE obtained as the resultant of the
energy balance ($LvE_{LAS} = R_n - G - H_{LAS}$).

On the other hand, one should mention that aggregation
procedures based on the flux matching rules do not deal di-
rectly with the primary surface variables, such as roughness
length and displacement height. In this context, and accord-
ing to previous study (Shuttleworth, 1988; Lagouarde et al.,
2002), a semi-empirical approach is generally used. It stipu-
lates that “the effective area-average value of land surface
parameters is estimated as a weighted average over the
component cover types in each grid through that function
involving the parameter which most succinctly expresses
its relationship with the associated surface flux”. Subse-
quently, in this context, the grid scale average displace-
ment height, $\langle d \rangle$, and roughness length, $\langle z_0 \rangle$, are
expressed as:

$$\langle d \rangle = f_c d_S + (1 - f_c) d_N \quad (15)$$

and

$$\left(\ln \left(\frac{z - \langle d \rangle}{\langle z_0 \rangle} \right) \right)^2 = f_c \left(\ln \left(\frac{z - d_S}{z_{0S}} \right) \right)^2 + (1 - f_c) \times \left(\ln \left(\frac{z - d_N}{z_{0N}} \right) \right)^2. \quad (16)$$

Here z_{0S} and z_{0N} represent the roughness length for the
southern and northern sites, respectively, each of which is
estimated as a fraction of the vegetation height (rule of
thumb).

374 Results and discussion

In this section, the closure of the energy balance of the
eddy-covariance data is analysed, followed by a comparison
between sensible heat fluxes measured by the EC systems
and by the LAS at patch scale. Thereafter we test the appli-
cability of MOST at grid scale when measurements are made
below the so-called blending height, followed by a compar-
ison of $\langle C_{nLAS}^2 \rangle_{\text{agg}}$ and $\langle C_{nEC}^2 \rangle_{\text{eff}}$ as well as a comparison be-
tween the LAS based and EC-based area-averaged sensible
heat flux. Note that only unstable conditions ($\frac{(z-d)}{L} < 0$) are
considered in this study.

385 Energy balance closure

As a measure of how the energy balance was closed in our
observations, the sum of the latent (LvE) and sensible (H)
heat fluxes derived from the EC system is balanced by the
available energy (net radiation (R_n) minus soil heat flux
(G)). The energy balance closure depends both on the
eddy-covariance measurements and the ability to ade-
quately quantify the available energy over an area represen-
tative of the flux source area. Most results in the literature
have shown the sum of sensible and latent heat fluxes mea-
sured by eddy-covariance to underestimate the available
energy (Twine et al., 2000; Hoedjes et al., 2002; Testi
et al., 2003).

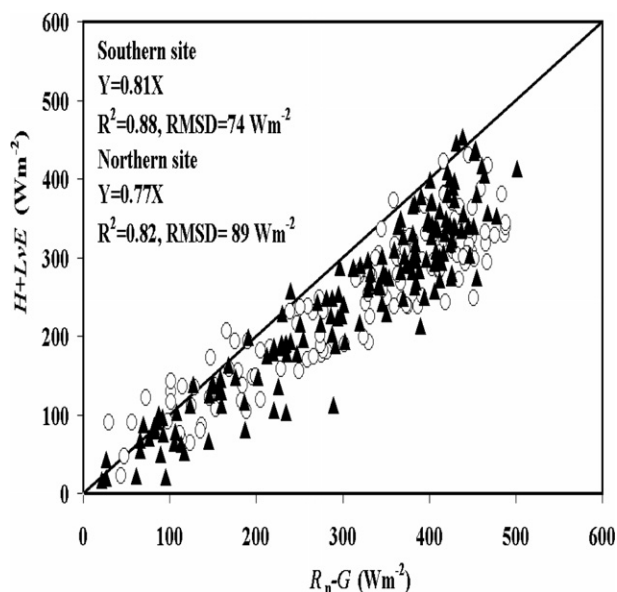


Figure 3 Comparison of half-hourly values of $H + L_vE$ and $R_n - G$ under unstable conditions, for northern site (triangles) and southern site (circles).

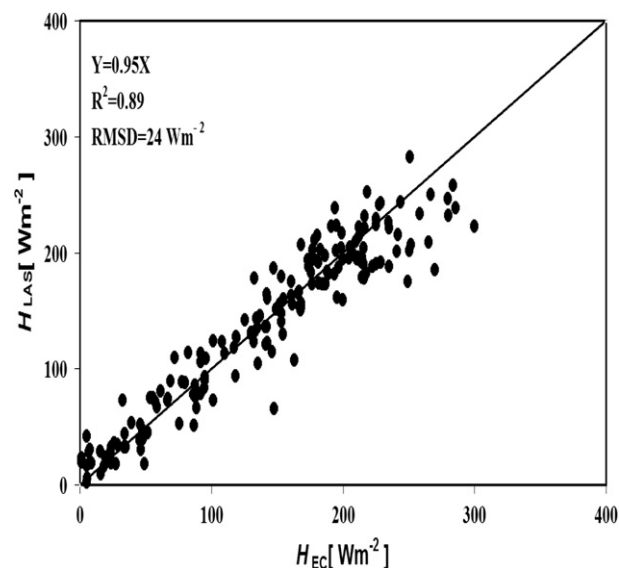


Figure 4a Comparison of H_{LAS} and H_{EC} during unstable conditions for the southern site.

398 **Fig. 3** shows the plots of $R_n - G$ against $H + L_vE$ for the
399 southern and northern sites. The linear regression (forced
400 through the origin) yields ($W m^{-2}$) $H_S + L_vE_S = 0.81(R_{nS} - G_S)$,
401 $R^2 = 0.88$ and the root mean square difference
402 (RMSD) = $74 W m^{-2}$ for the southern site, and
403 $H_N + L_vE_N = 0.77(R_{nN} - G_N)$, $R^2 = 0.82$ and RMSD = $89 W m^{-2}$
404 for the northern site. Several reasons can be suggested to
405 explain the lack of energy balance closure, for example
406 underestimation of the fluxes measured with the eddy-
407 covariance system, which might be due to the attenuation
408 of the true turbulent signals at sufficiently high and low fre-
409 quencies (e.g., Moore, 1986) or the differences in source
410 area for convective fluxes and available energy. Addition-
411 ally, energy storage within the olive tree biomass and in
412 the air column beneath the net radiation measurement is
413 not included in the energy balance. Scott et al. (2003) esti-
414 mated the energy storage within the biomass in similar eco-
415 systems to be about 5–10% of the available energy, which
416 might explain some of the lack in energy balance closure.
417 However, when compared to results reported in other
418 experimental studies (the average error in closure ranges
419 from 10% to 30% according to Twine et al., 2000), the energy
420 balance closure obtained here can be considered
421 acceptable.

422 Patch scale

423 In **Figs. 4a and 4b** the sensible heat fluxes obtained from the
424 LAS (H_{LAS}) are compared, under unstable conditions, to
425 those measured with eddy-covariance (H_{EC}) for the southern
426 and northern sites, respectively. For the southern site, linear
427 regression (forced through the origin) yields ($W m^{-2}$):
428 $H_{LAS,S} = 0.95H_{EC,S}$, $R^2 = 0.89$ and RMSD = $24 W m^{-2}$, and
429 $H_{LAS,N} = H_{EC,N}$, $R^2 = 0.74$ and RMSD = $27 W m^{-2}$ for the north-
430 ern site. The contrast between the two sites in terms of
431 water availability (irrigation) can clearly be seen in these

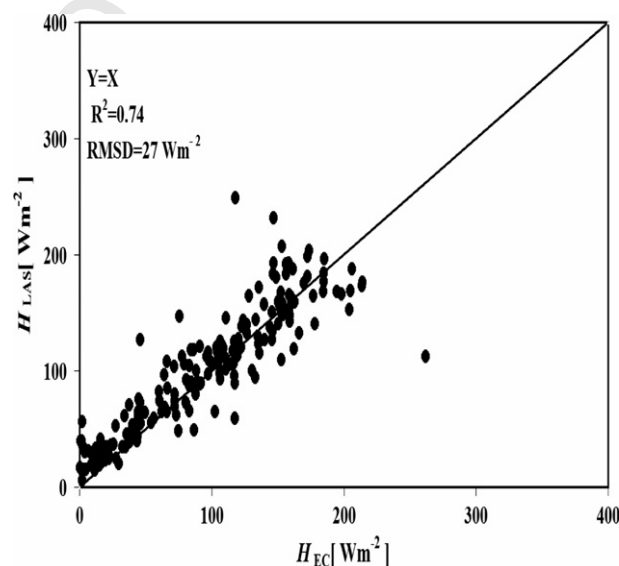


Figure 4b Comparison of H_{LAS} and H_{EC} during unstable conditions for the northern site.

figures. Sensible heat flux values over the southern site are considerably higher than those over the northern site. In the southern site, the maximum value of H was around $300 W m^{-2}$, while for the northern site the maximum was around $200 W m^{-2}$. The comparison shows a better agreement for the southern site than for the northern site. There are several explanations for the scatter in **Figs. 4a and 4b**. During some of the intervals used in this study, conditions were partly cloudy. Additionally, an irrigation event had taken place just before the experiment, with irrigation reaching the location of the EC-system on DOY 291. This caused heterogeneity in terms of soil moisture in the northern site during the experimental period. The impact of this heterogeneity is amplified by the differences in the source area of

446 the LAS and that of the EC system. Indeed, due to the flood
447 irrigation method employed in the site, it takes approxi-
448 mately 15 days to irrigate the entire field. During this peri-
449 od, the source area of the EC might be wet (dry) while a
450 significant portion of that of the LAS is dry (wet).

451 Grid scale

452 In order to derive fluxes from LAS one has to rely on the
453 Monin–Obukhov similarity theory (MOST). Since MOST re-
454 quires horizontal homogeneity, the question is whether this
455 theory still applies under heterogeneous conditions. Addi-
456 tionally, the measurements should be made above the
457 blending height, which depends according to Wieringa
458 (1986) on the friction velocity, wind speed and the horizon-
459 tal length scale of the heterogeneities. Under the prevailing
460 conditions over our study site, the average blending height
461 was at about 26 m at the grid scale. Unfortunately, the
462 operational deployment of the instruments at such height
463 is not feasible. It is therefore of interest to investigate
464 whether MOST holds under conditions of horizontal hetero-
465 geneity (at grid scale) where the measurements are made
466 below the blending height.

467 $\langle C_{nLAS}^2 \rangle_{agg}$ has been obtained assuming the linearity of scal-
468 ars fluxes derived from the LAS (sensible heat and momen-
469 tum fluxes over each field) using Eq. (11). In contrast to
470 Lagouarde et al. (2002), who simulated values of $\langle C_n^2 \rangle$ over
471 a two-surface composite landscape by weighting values of
472 C_n^2 computed for each field from the sensible heat flux
473 (eddy-covariance) according to the scintillometer weighting
474 function, here $\langle C_{nLAS}^2 \rangle_{agg}$ was directly derived using C_n^2 from
475 the LAS using Eq. (11) so that the non-linearity of C_n^2 is
476 avoided in the calculation of $\langle C_{nLAS}^2 \rangle_{agg}$.

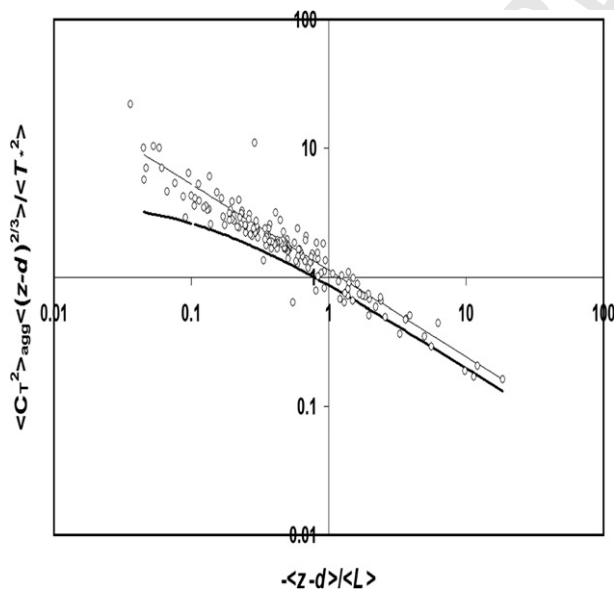


Figure 5 $\langle C_T^2 \rangle_{agg} \langle (z-d)^{2/3} \rangle / \langle T_*^2 \rangle$ plotted against $-(z-d)/\langle L \rangle$ during unstable conditions. Thick solid line represents the unstable scaling function found by de Bruin et al. (1993); also shown is the free convection relationship found by de Bruin et al. (1993): $f((z-d)/L) = 1.13(-(z-d)/L)^{-2/3}$ (solid line).

To check whether $\langle C_{TLAS}^2 \rangle_{agg}$, calculated from $\langle C_{nLAS}^2 \rangle_{agg}$ using Eq. (1), behaves according to MOST, we present in Fig. 5 a cross plot of $\langle C_{TLAS}^2 \rangle_{agg} \langle (z-d)^{2/3} \rangle / \langle T_*^2 \rangle$ and $\langle (z-d)/\langle L \rangle$. In order to avoid self-correlation due to MOST already being taken into account during the iterative procedure (Eqs. (1)–(5)), the effective values of $\langle \beta \rangle$, $\langle T_* \rangle$ and $\langle L \rangle$ have been constructed using solely eddy-covariance measurements. The result shows that the MOST scaling reported by de Bruin et al. (1993) still holds for heterogeneous surfaces, even though a small overestimation can be observed. Similar results have been found by Meijninger et al. (2002), who used the same scaling. These results confirm that MOST can be used below the blending height. This finding is in agreement with other studies (Shuttleworth, 1988; de Bruin, 1989; Ronda and de Bruin, 1999) which have shown that for surfaces with disorganized heterogeneity there is a layer below the blending height where MOST applies, but where contributions from separate fields can still be “seen”. In the same vein, Kohsiek et al. (2002) reported that when deploying the XLAS (extra large aperture scintillometer, which can be used over pathlengths of up to 10 km) below the blending, the violation of MOST is negligible. This is of interest since the operational deployment of an XLAS over a distance up of 10 km at or above the blending height is just not feasible.

Since both EC systems have been installed at approximately the same height above the canopy, it is safe to assume that each EC system has a similar sized source area, and therefore $f_{IEC} = 0.5$ in Eq. (6). For the LAS however, since the two scintillometers are not set up with the same orientation, depending on the wind direction, large differences can occur between the dimensions of the source area of each LAS. Therefore, the effect of changing of f_c on the aggregation model has been investigated by varying f_c between 0.1 and 0.9. Statistical results for a comparison between $\langle C_{nLAS}^2 \rangle_{agg}$ and $\langle C_{nEC}^2 \rangle_{eff}$, in order to check the sensitivity to the composition of the surface on $\langle C_{nLAS}^2 \rangle_{agg}$, are presented in Table 1. It shows that for the experimental site, to a good approximation, $f_c = 0.5$. In Fig. 6, a comparison between $\langle C_{nLAS}^2 \rangle_{agg}$ and $\langle C_{nEC}^2 \rangle_{eff}$ with $f_c = 0.5$ for cloud free days is presented. The comparison is good, with $R^2 = 0.95$ and the RMSD = $5 \times 10^{-15} \text{ m}^{-2/3}$. Note that the difference between the statistical results for $f_c = 0.5$ as shown in Table 1 and in Fig. 6 is caused by the exclusion of cloudy intervals in the data used in Fig. 6.

Finally, in Fig. 7 the grid scale sensible heat flux ($\langle H_{LAS} \rangle_{agg}$) simulated from $\langle C_{nLAS}^2 \rangle_{agg}$ (using Eqs. (1)–(5)) is compared with the area-average sensible heat fluxes $\langle H_{EC} \rangle_w$ defined as the linear weighing of sensible heat fluxes observed by the EC-systems of both fields with $f_c = f_{IEC} = 0.5$. The linear regression (forced through the origin) yields $\langle H_{LAS} \rangle_{agg} = \langle H_{EC} \rangle_w$, $R^2 = 0.89$ and RMSD = 20.3 W m^{-2} . This result shows less scatter than the comparison at patch scale, and correlation is good.

In the present experimental setup, no third scintillometer has been installed over the two patches (and above the blending height) for validation. Besides practical constraints, it should be noted that it is practically impossible to have a source area that matches the ensemble of the source areas of the two LAS installed at the individual patches. This scintillometer would have a varying contribution of the southern and northern sites, depending on wind

Table 1 Statistical results of the linear regression (forced through the origin) between simulated effective grid average $\langle C_{nLAS}^2 \rangle_{agg}$ with f_c (the fraction of the source area of LAS_s in the entire grid surface) varying between 0.1 and 0.9, and $\langle C_{nEC}^2 \rangle_{eff}$ with $f_{IEC} = 0.5$

Portion of south surface (f_c)	Slope	Correlation coefficient	RMSD $\times 10^{15}$ ($m^{-2/3}$)
0.1	0.77	0.8	12.8
0.2	0.83	0.83	10.8
0.3	0.89	0.85	9.1
0.4	0.95	0.87	8.2
0.5	1	0.88	7.8
0.6	1.07	0.88	8.78
0.7	1.14	0.87	10.6
0.8	1.2	0.87	13
0.9	1.27	0.86	16

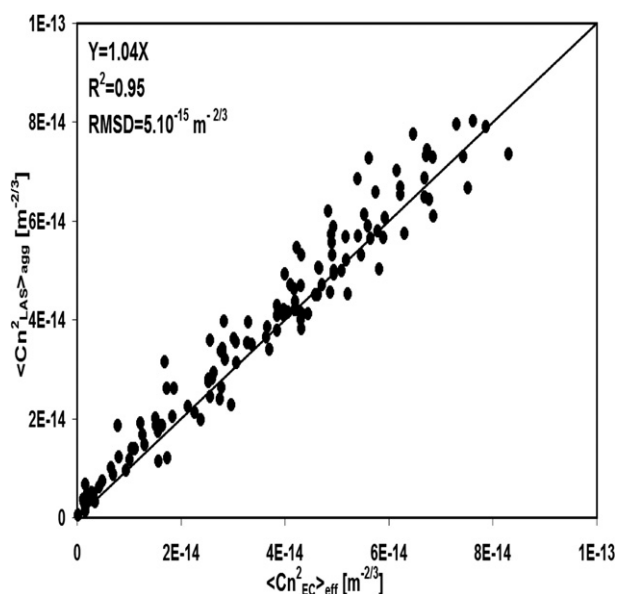


Figure 6 Comparison of $\langle C_{nLAS}^2 \rangle_{agg}$ obtained from the aggregation model and $\langle C_{nEC}^2 \rangle_{eff}$ obtained from $\langle H_{EC} \rangle_W$, $\langle LvE_{EC} \rangle_W$ and $\langle L_{EC} \rangle$; intervals without cloud passes.

539 direction, which will differ considerably from f_c . Therefore,
540 a third LAS does not provide a measurement that can be
541 used to validate the aggregation method developed in this
542 study.

543 Summary and conclusions

544 The general objective of the present study is to investigate
545 the applicability of MOST at grid scale (i.e., the combination
546 of the several individual fields, or patches). This is done by
547 combining the LAS measurements over two individual
548 patches with an aggregation scheme to infer the grid averaged
549 refractive index structure parameter $\langle C_n^2 \rangle$.

550 The comparisons between the half-hourly sensible heat
551 fluxes obtained from eddy-covariance and LAS at patch

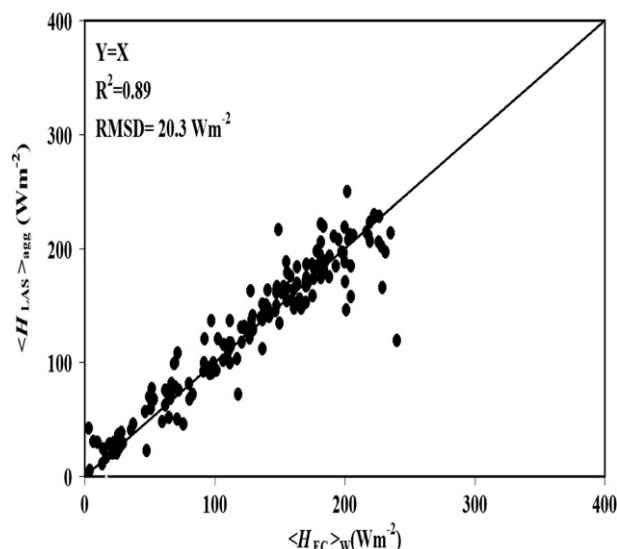


Figure 7 Comparison of grid scale sensible heat flux $\langle H_{LAS} \rangle_{agg}$ simulated from $\langle C_{nLAS}^2 \rangle_{agg}$ and $\langle H_{EC} \rangle_W$ derived by weighing the sensible heat fluxes observed from the EC-systems of both fields ($f_c = f_{IEC} = 0.5$).

scale yield a good result. The RMSD is 24.5 and 28.3 $W m^{-2}$ for the southern and northern sites, respectively. The difference in flux between the two fields is mainly caused by an irrigation event which took place in the northern site during the experiment. This also explains part of the scatter and lower correlation between H_{EC} and H_{LAS} for the northern site, since during irrigation, the impact of the differences in the source areas of the two instruments increased significantly. However, despite some scatter, it can be assumed that MOST is applicable over relatively tall and sparse trees. Furthermore, the two comparisons show the difference between the two sites at the time of the experiment. Consequently, the grid, comprised of the two patches, can be considered as heterogeneous.

A combination of patch scale LAS measurements, meteorological data and an aggregation model have been used to derive a grid averaged $\langle C_{nLAS}^2 \rangle_{agg}$, from which the grid averaged structure parameter of temperature is calculated. This $\langle C_{TLAS}^2 \rangle_{agg}$ is shown to behave according to MOST, although some scatter is observed. However, this scatter can be considered acceptable (see for example Beljaars et al., 1983; Weaver, 1990; de Bruin et al., 1993), and therefore MOST is considered to be applicable at grid scale, even when the measurements have been taken below the blending height.

There are practical constraints for the installation of a third scintillometer to measure over the entire grid; to overcome saturation and to be above the blending height (see for example Meijninger et al., 2002), one would have to install this third scintillometer much higher than the two LAS in used in this study. Therefore, in order to verify the accuracy of the values of $\langle C_{nLAS}^2 \rangle_{agg}$, an effective parameter has been used. This effective approach uses averages of friction velocity and sensible and latent heat fluxes from the EC system in combination with MOST to calculate $\langle C_n^2 \rangle$ values. In the case where MOST is applicable, this would be the grid-scale value of C_n^2 , and this $\langle C_n^2 \rangle_{eff}$ can therefore be used to

552
553
554
555
556
557
558
559
560
561
562
563
564
565
566
567
568
569
570
571
572
573
574
575
576
577
578
579
580
581
582
583
584
585
586
587
588

589 validate $\langle C_{nLAS}^2 \rangle_{agg}$. Despite some scatter, the comparison is
590 good which confirms the consistency of the aggregation
591 method.

592 The results of this study demonstrate the applicability of
593 the LAS and thus the XLAS, over large and heterogeneous
594 grids when deployed below the blending height. Conse-
595 quently, the minimum height at which a scintillometer can
596 be operated is not the blending height, but the height below
597 which saturation of the signal occurs (see for example
598 Moene et al., 2005). Furthermore, since available energy
599 is easily obtained from spaceborne sensors, e.g. Meteosat
600 Second Generation or MODIS (<http://postel.obs-mip.fr/postel/>),
601 this allows the determination of evapotranspiration
602 at the aforementioned scales, which can be used for
603 e.g. irrigation monitoring, or the validation of mesoscale
604 atmospheric models or hydrological models.

605 Acknowledgements

606 This research was situated within the framework of SUD-
607 MED, U.E. funded IRRIMED (<http://www.irrimed.org>) and
608 Pleiades projects. We are grateful to the Institut de Recher-
609 che pour le Développement (IRD, France), the Department
610 of Meteorology and Air Quality of Wageningen University
611 (The Netherlands) and the PNTS (Programme National de
612 Télédétection Spatiale, France). We are indebted to the
613 director and staff of the Agdal olive orchard for access
614 and use of the field site and for assistance with irrigation
615 scheduling and security. Many thanks to O.K. Hartogensis
616 for his technical assistance during the field experiment,
617 especially on the preparation of the experiment and the
618 installation of the EC-systems. During the experiment,
619 J.C.B. Hoedjes was supported by a fellowship from STW,
620 The Netherlands (project no. WMO4133).

621 References

- 622 Arain, A.M., Michaud, J.D., Shuttleworth, W.J., Dolman, A.J., 1996.
623 Testing of vegetation parameter aggregation rules applicable to
624 the biosphere-atmosphere transfer scheme (BATS) at the FIFE
625 site. *J. Hydrol.* 177, 1–22.
- 626 Beljaars, A.C.M., Schotanus, P., Nieuwstadt, F.T.M., 1983. Surface
627 layer similarity under nonuniform fetch conditions. *J. Clim.*
628 *Appl. Meteorol.* 22, 1800–1810.
- 629 Beyrich, F., de Bruin, H.A.R., Meijninger, W.M.L., Schipper, J.W.,
630 Lohse, H., 2002. Results from one-year continuous operation of
631 a large aperture scintillometer over a heterogeneous land
632 surface. *Boundary-Layer Meteorol.* 105, 85–97.
- 633 Chehbouni, A., Escadafal, R., Dedieu, G., Errouane, S., Boulet, G.,
634 Duchemin, B., Mougnot, B., Simonneaux, V., Seghieri, J.,
635 Timouk, F., 2003. A multidisciplinary program for assessing the
636 sustainability of water resources in semi-arid basin in Morocco:
637 SUDMED. EGS-AGU-EUG Joint Assembly, April 6–11, 2003, Nice
638 (France).
- 639 Chehbouni, A., Watts, C., Kerr, Y.H., Dedieu, G., Rodriguez, J.-C.,
640 Santiago, F., Cayrol, P., Boulet, G., Goodrich, D.C., 2000a.
641 Methods to aggregate turbulent fluxes over heterogeneous
642 surfaces: application to SALSA data set in Mexico. *Agric. Forest*
643 *Meteorol.* 105, 133–144.
- 644 Chehbouni, A., Watts, C., Lagouarde, J.-P., Kerr, Y.H., Rodriguez,
645 J.-C., Bonnefond, J.-M., Santiago, F., Dedieu, G., Goodrich,
646 D.C., Unkrich, C., 2000b. Estimation of heat fluxes and momen-

- tum fluxes over complex terrain using a large aperture scintil-
lometer. *Agric. Forest Meteorol.* 105, 215–226. 647
648
- Chehbouni, A., Kerr, Y.H., Watts, C., Hartogensis, O.K., Goodrich,
D.C., Scott, R., Schieldge, J., Lee, K., Shuttleworth, W.J.,
Dedieu, G., de Bruin, H.A.R., 1999. Estimation of area-average
sensible heat flux using a large aperture scintillometer. *Water*
Resour. Res. 35, 215–226. 649
650
651
652
653
- Chehbouni, A., Njoku, E.G., Lhomme, J.-P., Kerr, Y.H., 1995. An
approach for averaging surface temperature and surface fluxes
over heterogeneous surfaces. *J. Climate* 5, 1386–1393. 654
655
656
- de Bruin, H.A.R., van den Hurk, B.J.J.M., Kohsiek, W., 1995. The
scintillation method tested over a dry vineyard area. *Boundary-*
Layer Meteorol. 76, 25–40. 657
658
659
- de Bruin, H.A.R., Kohsiek, W., van den Hurk, B.J.J.M., 1993. A
verification of some methods to determine the fluxes of
momentum, sensible heat and water vapour using standard
deviation and structure parameter of scalar meteorological
quantities. *Boundary-Layer Meteorol.* 76, 25–40. 660
661
662
663
664
- de Bruin, H.A.R., 1989. Physical aspects of the planetary boundary
layer with special reference to regional evapotranspiration. In:
Proc. Workshop on the Estimation of Areal Evapotranspiration,
Vancouver, BC, August, 1987. IAHS Publ., 177, pp. 117–132. 665
666
667
668
- Green, A.E., McAneney, K.J., Astill, M.S., 1994. Surface layer
scintillation measurements of daytime heat and momentum
fluxes. *Boundary-Layer Meteorol.* 68, 357–373. 669
670
671
- Hoedjes, J.C.B., Zuurbier, R.M., Watts, C.J., 2002. Large aperture
scintillometer used over a homogeneous irrigated area, partly
affected by regional advection. *Boundary-Layer Meteorol.* 105,
99–117. 672
673
674
675
- Kohsiek, W., Meijninger, W.M.L., Moene, A.F., Heusinkveld, B.G.,
Hartogensis, O.K., Hillen, W.C.A.M., de Bruin, H.A.R., 2002. An
extra large aperture scintillometer (XLAS) with a 9.8 km path
length. *Boundary-Layer Meteorol.* 105, 119–127. 676
677
678
679
- Lagouarde, J.-P., Bonnefond, J.-M., Kerr, Y.H., McAneney, K.J.,
Irvine, M., 2002. Integrated sensible heat flux measurements of
a two-surface composite landscape using scintillometry. *Bound-*
ary-Layer Meteorol. 105, 5–35. 680
681
682
683
- Meijninger, W.M.L., de Bruin, H.A.R., 2000. The sensible heat flux
over irrigated area in western Turkey determined with a large
aperture scintillometer. *J. Hydrol.* 229, 42–49. 684
685
686
- Meijninger, W.M.L., Hartogensis, O.K., Kohsiek, W., Hoedjes,
J.C.B., Zuurbier, R.M., de Bruin, H.A.R., 2002. Determination
of area-averaged sensible heat fluxes with a large aperture
scintillometer over a heterogeneous surface – Flevoland field
experiment. *Boundary-Layer Meteorol.* 105, 37–62. 687
688
689
690
691
- Moene, A.F., 2003. Effects of water vapour on the structure
parameter of the refractive index for near-infrared radiation.
Boundary-Layer Meteorol. 107, 635–653. 692
693
694
- Moene, A.F., Meijninger, W.M.L., Hartogensis, O.K., Kohsiek, W., de
Bruin, H.A.R., 2005. A review of the relationships describing the
signal of a Large Aperture Scintillometer. Internal Report 2004/
2, Updated Version 1.1, Meteorology and Air Quality Group,
Wageningen University, Wageningen, The Netherlands, 39pp. 695
696
697
698
699
- Moore, C.J., 1986. Frequency response corrections for eddy-
correlation systems. *Boundary-Layer Meteorol.* 37, 17–
35. 700
701
702
- Noilhan, J., Lacarrere, L., 1995. GCM grid scale evaporation from
mesoscale modelling: a method based on parameter aggregation
tested for clear days of Hapex-Mobilhy. *J. Climate* 8, 206–223. 703
704
705
- Ochs, G.R., Wilson, J.J., 1993. A second-generation large-aperture
scintillometer. NOAA Tech. Memo, ERL WPL-232, NOAA Envi-
ronmental Research Laboratories, Boulder, CO, 24pp. 706
707
708
- Panofsky, H.A., Dutton, J.A., 1984. *Atmospheric Turbulence:*
Models and Methods for Engineering Applications. Wiley, New
York, 397pp. 709
710
711
- Ronda, R.J., de Bruin, H.A.R., 1999. A note on the concept of
'effective' bulk exchange coefficients for determination of
surface flux densities. *Boundary-Layer Meteorol.* 93, 155–162. 712
713
714

715	Scott, R.W.C., Garatuza-Payan, J., Edwards, E., Goodrich, D.C.,	731
716	Williams, D.G., Shuttleworth, W.J., 2003. The understory and	732
717	overstory partitioning of energy and water fluxes in an open	733
718	canopy, semi-arid woodland. <i>Agric. Forest Meteorol.</i> 114, 127–	734
719	139.	735
720	Shuttleworth, W.J., 1991. The modellion concept. <i>Rev. Geophys.</i>	736
721	29, 585–606.	737
722	Shuttleworth, W.J., 1988. Macrohydrology – The new challenge for	738
723	process hydrology. <i>J. Hydrol.</i> 100, 31–56.	739
724	Twine, T.E., Kustas, W.P., Norman, J.M., Cook, D.R., Houser, P.R.,	740
725	Meyers, T.P., Prueger, J.H., Starks, P.J., Wesely, M.L., 2000.	741
726	Correcting eddy-covariance flux underestimates over a grass-	742
727	land. <i>Agric. Forest Meteorol.</i> 103, 279–300.	743
728	Testi, L., Villalobos, F.J., Orgaz, F., 2003. Evapotranspiration of a	744
729	young irrigated olive orchard in southern Spain. <i>Agric. Forest</i>	745
730	<i>Meteorol.</i> 121, 1–18.	746
	Wang, T., Ochs, G.R., Clifford, S.F., 1978. A saturation resistant	
	optical scintillometer to measure C_n^2 . <i>J. Opt. Soc. Am.</i> 68, 334–	
	338.	
	Weaver, H.L., 1990. Temperature and humidity flux-variance	
	relations determined by one-dimensional eddy correlations.	
	<i>Boundary-Layer Meteorol.</i> 53, 77–91.	
	Webb, E.K., Pearman, G.I., Leuning, R., 1980. Correction of flux	
	measurements for density effects due to heat and water vapor	
	transfer. <i>Quart. J. Roy. Meteorol. Soc.</i> 106, 85–100.	
	Wesely, M.L., 1976. The combined effect of temperature and	
	humidity fluctuations on refractive index. <i>J. Appl. Meteorol.</i> 15,	
	43–49.	
	Wieringa, J., 1986. Roughness dependent geographical interpola-	
	tion of surface wind speed averages. <i>Quart. J. Roy. Meteorol.</i>	
	<i>Soc.</i> 112, 867–889.	

UNCORRECTED PROOF